We are IntechOpen,
the world's leading publisher of
Open Access books
Built by scientists, for scientists

6,900
Open access books available

185,000
International authors and editors

200M
Downloads

154
Countries delivered to

Our authors are among the

TOP 1%
most cited scientists

12.2%
Contributors from top 500 universities

CLARIVATE ANALYTICS
BOOK CITATION INDEX
INDEXED

WEB OF SCIENCE™

Selection of our books indexed in the Book Citation Index
in Web of Science™ Core Collection (BKCI)

Interested in publishing with us?
Contact book.department@intechopen.com

Ga$_2$O$_3$ Nanowire Synthesis and Device Applications

Badriyah Alhalaili, Howard Mao and Saif Islam

Additional information is available at the end of the chapter

Abstract

In recent years, gallium oxide nanowires have been used in many scientific disciplines due to their outstanding and unique properties. Several applications have focused on incorporating gallium oxide nanowires in devices to improve their performance and efficiency. These distinctive structures bring new opportunities to several research fields and applications such as optoelectronics, electronics, and chemistry. This chapter provides a basic overview of gallium oxide's properties and the growth process of gallium oxide nanowires, with an emphasis on varied applications and future challenges.

Keywords: β-Ga$_2$O$_3$ nanowires, properties, growth, nanodevices, applications, challenges

1. Introduction

In the last few years, interest in the use of wide-bandgap materials in semiconductor devices has grown. Ideally, such materials would be abundant, inexpensive, and easy to fabricate, and have high thermal and chemical stability. However, reducing the size of these materials and the devices that utilize them down to the micro/nanoscale remains a big challenge. Furthermore, manipulating their growth to create more directional nanowires could be useful in several applications. In addition, a limited number of devices such as transistors and sensors are capable of operating at temperatures up to 500°C. Wide-bandgap materials can operate in harsh environmental conditions with high temperature, pressure, mechanical vibration and radiation. Therefore, sensors and electronic devices incorporating these materials are attractive choices for increasing the operating temperature to above 500°C while effectively integrating electronics operating even at 1000°C [1].

Preliminary studies demonstrate that some robust wide-bandgap materials can enable a number of devices and sensors that can be used in extreme environments [1, 2]. These benefits can
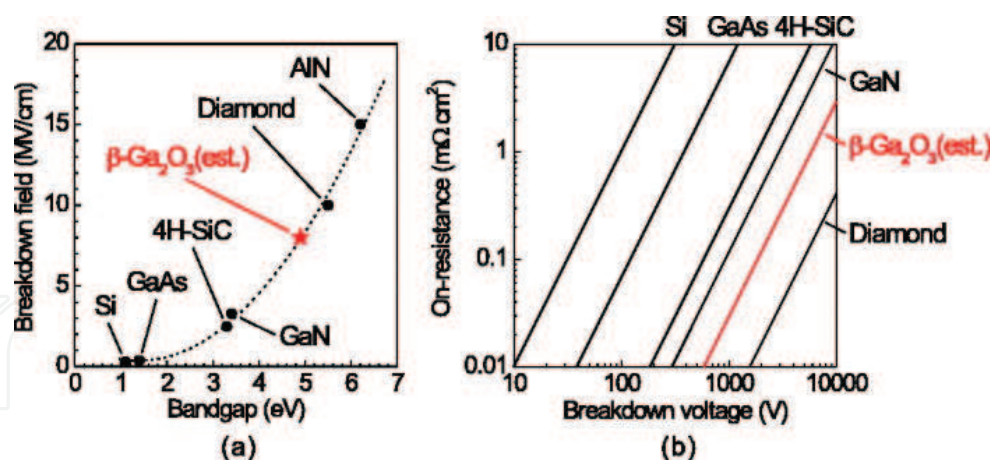
Figure 1. (a) Relationship between the bandgap and breakdown field for various semiconductor materials, (b) On-resistance as a function of breakdown voltage for major semiconductors. (Reprinted with permission from [82]. Copyright 2012, American Institute of Physics.).

be realized by exploiting the electrical, optical, thermal, physical and chemical properties of wide-bandgap semiconductors including group III nitrides such as gallium nitride (GaN), aluminum nitride (AlN) and their ternary and quaternary alloys; and silicon carbide (SiC), diamond and some wide-bandgap oxides (such as Ga_2O_3). These materials offer superior electrical, optical, mechanical, and chemical properties when compared to other widely used semiconductor materials such as Si, GaAs and InP [1, 3].

Gallium oxide has a promising future with respect to other semiconductors based on its material properties (**Figure 1a**). It has the potential to be more widely used in power and optoelectronics applications than not only Si but also SiC and GaN. This is due to its high breakdown voltage and low on-resistance (**Figure 1b**). These features have led to the evaluation of Ga_2O_3 nanowires as a novel material in semiconductor research fields; it is also less expensive and easier to fabricate than SiC and GaN. Compared to thin films, nanowires have a higher surface-to-volume ratio, which increases their sensitivity in detection. Ga_2O_3 nanowires have an established place in many applications, such as optical and sensing studies [4, 5]. For example, $β$-Ga_2O_3 nanowire-based devices are very attractive for use as gas sensors [6] due to their stability, moisture resistance, fast response, and long lifetime. Research interest in Ga_2O_3 nanowires has been increasing, and it has obtained recognition among other wide-bandgap materials. This chapter will mainly focus on synthesis techniques, device applications, and future challenges for $β$-Ga_2O_3 nanowires.

2. Fundamental properties of $β$-Ga_2O_3 nanowires

Gallium (III) oxide is an insulating metal oxide with five different polymorphs ($α$-, $β$- $γ$-, $δ$-, $ε$-). $β$-Ga_2O_3 has a monoclinic structure and is the most stable form both chemically and thermally. The other phases exist in a metastable state and are converted into $β$-phase at temperatures above 600°C. $β$-Ga_2O_3 has exceptional properties which have attracted the attention of scientists, including a wide bandgap of 4.9 eV, a high melting point of 1900°C, excellent electrical conductivity, and photoluminescence. Despite these wonderful properties, it is only in recent years that interest in this material has grown.

Recently, researchers have showed interest in the fabrication of low-dimensional β-Ga$_2$O$_3$ nanowires because of their outstanding properties as compared to bulk structures. The main advantage of β-Ga$_2$O$_3$ nanowires is a higher surface-to-volume ratio, offering more surface states at the interface and thus greater interaction with the surroundings. β-Ga$_2$O$_3$ nanowires can be synthesized using a variety of approaches, and various parameters such as size, length and electronic properties can be controlled during their growth. Recently, a wide array of nanoscale devices such as FETs, gas sensors, photodetectors, and nanophotonic switches have been fabricated using β-Ga$_2$O$_3$ nanowires. These β-Ga$_2$O$_3$ nanowire devices are also popular for diverse applications such as displays [7], solar cell fabrication [8], ultraviolet (UV) limiters [9], and high-temperature gas sensors [10].

2.1. Crystal structure

In 1950, Ga$_2$O$_3$ was observed, and in 1960, its crystal structure was discovered by Geller [7]. β-Ga$_2$O$_3$ is part of the C2/m space group and has a base-centered arrangement with four lattice parameters (**Table 1**). The unit cell of β-Ga$_2$O$_3$ has two different Ga atoms [Ga(I) and Ga(II)] and three different O atoms [O(I), O(II) and O(III)] (**Figure 2**). The crystalline structures that make up the unit cell are octahedral (GaO$_6$) and tetrahedral (GaO$_4$). Along the b-axis, the double-chained GaO$_6$ octahedra that share edges are connected by single chains of GaO$_4$ tetrahedra that share vertices. The unit cell consists of three different oxygen ions that are juxtaposed in an irregular cubic array and are close to one another.

2.2. Electrical properties

2.2.1. Energy bandgap for Ga$_2$O$_3$

Density functional theory (DFT) has been used to calculate the electronic band structure of β-Ga$_2$O$_3$. β-Ga$_2$O$_3$ has an indirect bandgap of 4.83 eV, with a valence-band maximum (VBM) located at the M point, which is marginally less than the direct bandgap of 4.87 eV detected at the Γ-point, as shown in **Figure 3** [11]. Research has confirmed that β-Ga$_2$O$_3$ is an indirect bandgap material, but due to the weakness of the indirect transitions and the small energy difference between indirect and direct gaps, it is effectively a direct bandgap material. Peak absorption occurs around 4.9 eV. **Table 1** summarizes the electronic properties of β-Ga$_2$O$_3$.

2.2.2. Dopants for Ga$_2$O$_3$

As Ga$_2$O$_3$ is an insulator, it needs to be doped to increase its conductivity. Doping enables control of sheet resistance [12] and facilitates the formation of ohmic contacts. It can also change many properties of a material. For example, it can increase the lattice constant [13], and change crystallinity [14] and electron mobility [15]. Doping can even be used to tune the optical bandgap [16] and introduce defect levels [17]. It is typically done at the same time nanowires are grown, using methods such as chemical vapor deposition, pulsed laser deposition, and evaporation. Alternatively, dopants can be added directly into the material through ion implantation.

β-Ga$_2$O$_3$ is assumed to be an n-type semiconductor due to its shallow donor oxygen vacancies and ionization energy of 30–40 meV [9]. Its electrical conduction and free carrier concentration can be adjusted by doping it with Si. The effects of oxygen vacancies and other impurities on the electrical and optical properties of Ga$_2$O$_3$ have also been examined [11]. It was found that

Property	Attributes
Crystal structure	Monoclinic
Group of symmetry	C2/m
Lattice parameters	
a	12.214 Å
b	3.037 Å
c	5.798 Å
β	103.83 Å
Bandgap (E_g)	4.83 eV (indirect) & 4.87 (direct) at RT
Density	5.863 g/cm³
Dopants (n/p type)	Ti/Zn, Ge, Mg
Electron affinity (χ)	3.50 eV
Electron effective mass	$0.342m_e$
Electron mobility (μ_e)	10 cm² V⁻¹ s⁻¹
Carrier density	10^{13}–10^{16} cm⁻³
Rel. dielectric constant (ϵ)	9.9–10.2
Melting point	1800 °C
Specific heat	0.49–0.56 Jg⁻¹ K⁻¹
Thermal conductivity	
[100]	(10.9 ±1.0 W/mK)–(13 W/mK)
[−201]	13.3 ± 1.0 W/mK
[001]	14.7 ±1.5 W/mK
[110]	(27.0 ±2.0 W/mK)–(21 W/mK)
Refractive index (*n*) @ 532 nm	
∥[100]	1.9523
⊥(100)	1.9201

Table 1. Summary of the basic properties of β-Ga$_2$O$_3$ [18, 29].

it cannot be assumed that oxygen vacancies are the main cause for conduction and luminance because Si is the main impurity behind electrical conduction [18]. Furthermore, these oxygen vacancies are deep donors and hence cannot describe the n-type conductivity. Other dopants such as Si, Ge, Sn, F, and Cl behave like shallow donors. In the next sub-section, we describe some dopants and their properties. **Table 2** summarizes the materials that have been used as dopants for Ga$_2$O$_3$ and the changes they make to it.

2.2.2.1. Indium (In)

Indium is one dopant that can be used with Ga$_2$O$_3$ to improve its photoelectrical properties, especially in the context of photodetection [13]. Doping with indium narrows the bandgap, which increases the range of the photoresponse but makes the photodetector less sensitive
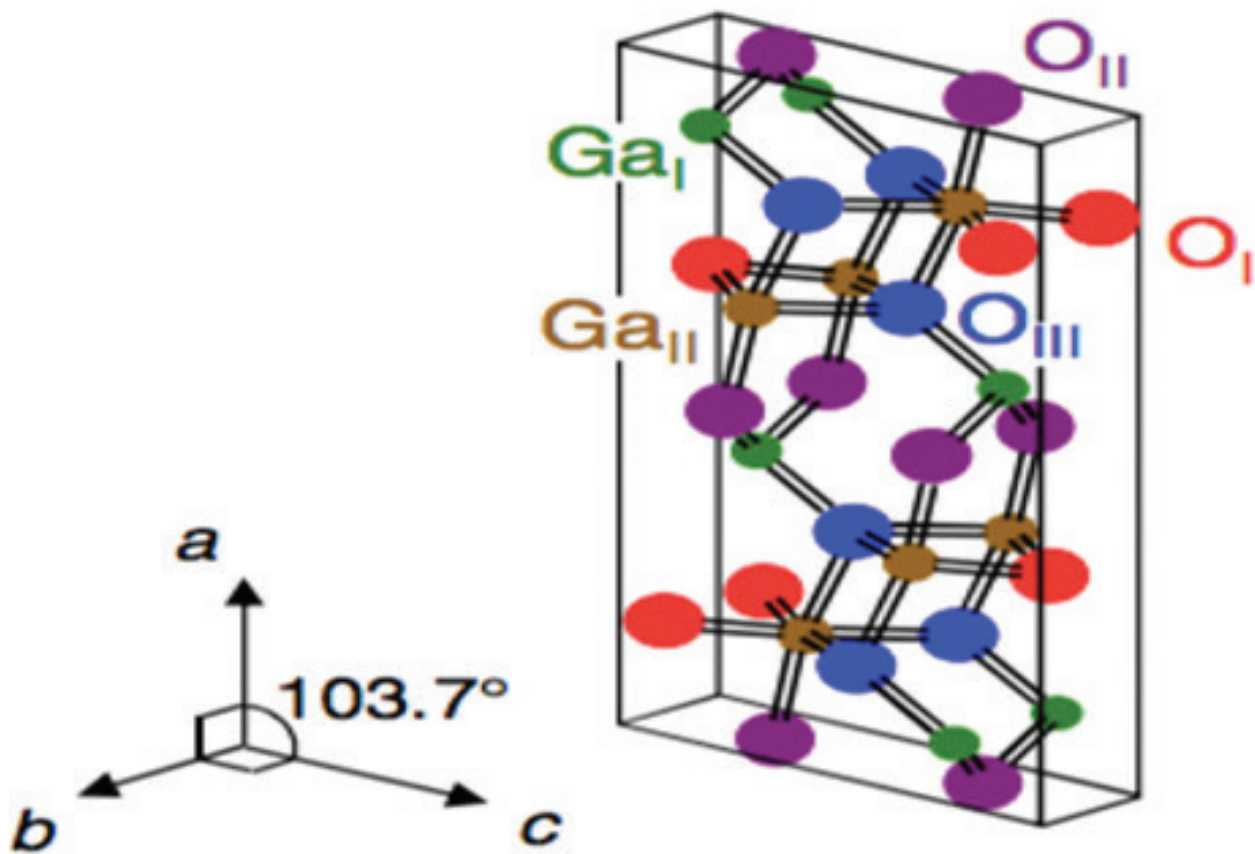
Figure 2. Unit cell of β-Ga$_2$O$_3$.

to UV wavelengths. Doping causes the photocurrent to be much larger than that of undoped devices. This is also true for the ratio of photocurrent to dark current. Indium doping can also reduce rise time and improve spectral responsivity and external quantum efficiency.

2.2.2.2. Silicon (Si)

Si has also been used to dope Ga$_2$O$_3$, significantly reducing its resistance after ion implantation of Si atoms and annealing [12]. Si doping also helps in creating an ohmic contact
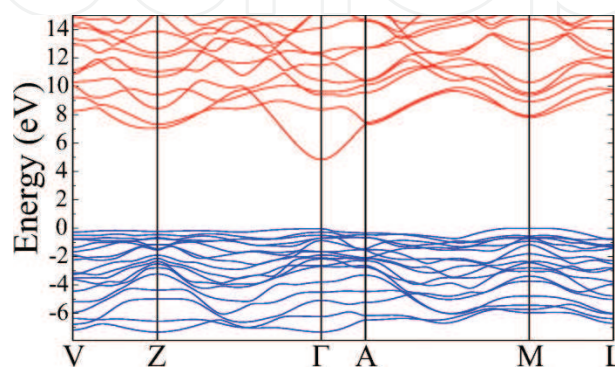

Figure 3. Electronic band structure of β-Ga$_2$O$_3$. (Reprinted with permission from Ref. [11]. Copyright 2010, American Institute of Physics.).

Materials	Properties
In	To improve the photoelectrical properties
Si	• To reduce sheet resistance of Ga_2O_3 • To support creating an ohmic contact on the surface
Sn	To increase conductivity.
Mg	A promise in making Ga_2O_3 p-type
Cu	• To decrease bandgap because CuO has a narrower bandgap than Ga_2O_3 • A potential to be a p-type dopant for Ga_2O_3
Zn	• A potential to be a p-type dopant for Ga_2O_3 • To decrease carrier concentration
Ti	• To decrease dielectric permittivity • To increase the optosensitivity • To reduce leakage current
N	Doping with N has the potential to make Ga_2O_3 p-type

Table 2. Some materials have been used as a dopant and their properties.

on the surface with Ti and Au. It was seen to increase the rejection ratio, photocurrent, responsivity, and quantum efficiency of a photodetector at high temperatures. γ-Ga_2O_3 has been doped n-type by ablation of a Ga_2O_3:Si ceramic target with laser pulses [19]. In that case, doping capability was independent of crystal structure, and carrier concentration did not vary much with temperature, meaning the Ga_2O_3 had been degenerately doped.

2.2.2.3. Tin (Sn)

Ga_2O_3 has also been doped with Sn to increase its conductivity [14]. Interestingly, when deposition was performed at temperatures above 410°C, doping caused the phase of the Ga_2O_3 to change from β-Ga_2O_3 to ε-Ga_2O_3. Another method of doping Ga_2O_3 with Sn is heating SnO_2 powder in a K-cell with ozone as an oxidizer [15]. However, it was observed that as the temperature of the SnO_2 powder was raised, the carrier concentration increased, which lowered electron mobility.

2.2.2.4. Magnesium (Mg)

Mg is one of a few materials believed to hold promise in making Ga_2O_3 p-type. Mg-doped Ga_2O_3 has been deposited into an MOCVD system with a Mg-containing source, and as the Mg concentration was increased from 1–10%, the crystalline quality degraded, with films becoming amorphous [16]. Annealing improved the crystallinity and lowered the resistivity, but the Ga_2O_3 did not become p-type as expected after doping.

2.2.2.5. Copper (Cu)

Ga_2O_3 has also been doped with Cu, which reduces the bandgap because CuO has a narrower bandgap than Ga_2O_3 [17]. The bandgap widens again after annealing. Ga^{3+} and Cu^{2+} have a similar ionic size (0.073 nm and 0.062 nm, respectively), and copper is a group IB element, so copper has the potential to be a p-type dopant for Ga_2O_3. Because Cu has fewer valence electrons than Ga does, there is a lower density of electrons between Cu and O than between Ga and O [20]. After doping, the acceptor impurity level in Ga_2O_3 is higher than the valence band.

2.2.2.6. Zinc (Zn)

Zn has potential to be used as a p-type dopant for Ga_2O_3 as it can add holes to the material after annealing and belongs to group IIB with one fewer valence electron than Ga_2O_3 [21]. While undoped β-Ga_2O_3 is clearly n-type, after doping with Zn the conductivity type could not be clearly determined because there were both electrons and holes and their concentrations were approximately equal. High transmittance was observed, indicating that crystalline quality was high. Adding Zn also caused the carrier concentration to drop from 1.4×10^{14} to 7.2×10^{11} cm^{-3}.

2.2.2.7. Titanium (Ti)

Doping Ga_2O_3 with Ti lowers its dielectric permittivity. [22]. Ti can dope about 10% of Ga_2O_3 due to their similar ionic radii (0.047 and 0.042 nm for Ga^{3+} and Ti^{4+}, respectively). This gives titanium ions high solubility in Ga_2O_3. Inclusion of Ti increases the optosensitivity of samples and reduces leakage current by increasing the activation energy and narrowing the bandgap.

2.2.2.8. Nitrogen (N)

N^{3-} has an ionic radius about the same as that of O^{2-}, so it can be expected to form shallow acceptor levels [23], which is significant because the difficulty of forming shallow acceptor levels in Ga_2O_3 is the main challenge in making it p-type. On doping Ga_2O_3 with N, the bandgap decreased and the valence band maximum and conduction band maximum met at the same point. The acceptor impurity levels were above the valence band. After Ga_2O_3 nanowires were doped with N, they exhibited p-type properties [24]. Pt has a larger work function than Ga_2O_3 and it was used for the metal contacts. When a contact metal has a work function larger than that of the semiconductor, a Schottky barrier is created when the semiconductor is n-type and an ohmic contact is exhibited for a p-type semiconductor. While an undoped Ga_2O_3 nanowire had an I-V characteristic that was rectifying, a N-doped nanowire had a linear I-V curve. This suggests that doping Ga_2O_3 with N can make it p-type.

2.3. Optical properties

2.3.1. Absorption of Ga_2O_3 nanowires

The absorption spectra of Ga_2O_3 show cutoff absorption edges at around 255–260 nm and slightly around 270 nm [18]. The band at 260 nm was due to the intrinsic band-to-band transition while the one at 270 nm was caused by Ga^{3+} vacancies in the conduction band. The

absorption range (255–260 nm) can be obtained because of the transition from the valence band to the conduction band [25]. The absorption of Ga_2O_3 is influenced by polarization of incident light [26]. The difference between the absorption edge at 260 and at 270 nm was attained using the transition from the valence band.

2.3.2. Luminescence properties of Ga_2O_3 nanowires

Ga_2O_3 can produce four emissions: UV (3.2–3.6 eV), blue (2.8–3.0 eV), green (2.4 eV) [27, 28] and red [29]. Due to its wide bandgap, there are a number of defect states, which cause its different emissions from infrared to UV because its wide bandgap has a number of defect states that are responsible for them. The bandgap of Ga_2O_3 is known to be 4.8 eV, suggesting that UV emission initiated from the edge of the band is due to free electrons and recombination of self-trapped holes [30]. However, the blue and deep-blue luminescence are caused by the recombination of an electron on a defect donor state formed by oxygen vacancies and a hole on an acceptor state formed by a gallium vacancy or a gallium–oxygen vacancy pair [28, 31]. Green emission could only be achieved when the samples were doped with certain impurities such as Be, Ge, Sn, Li, Zr, and Si [18, 32]. It has been suggested that green luminescence is related to self-trapped or bound excitons [26]. Several studies have been performed on the excitation and photoluminescence of pure and Si-doped β-Ga_2O_3 single crystals [33].
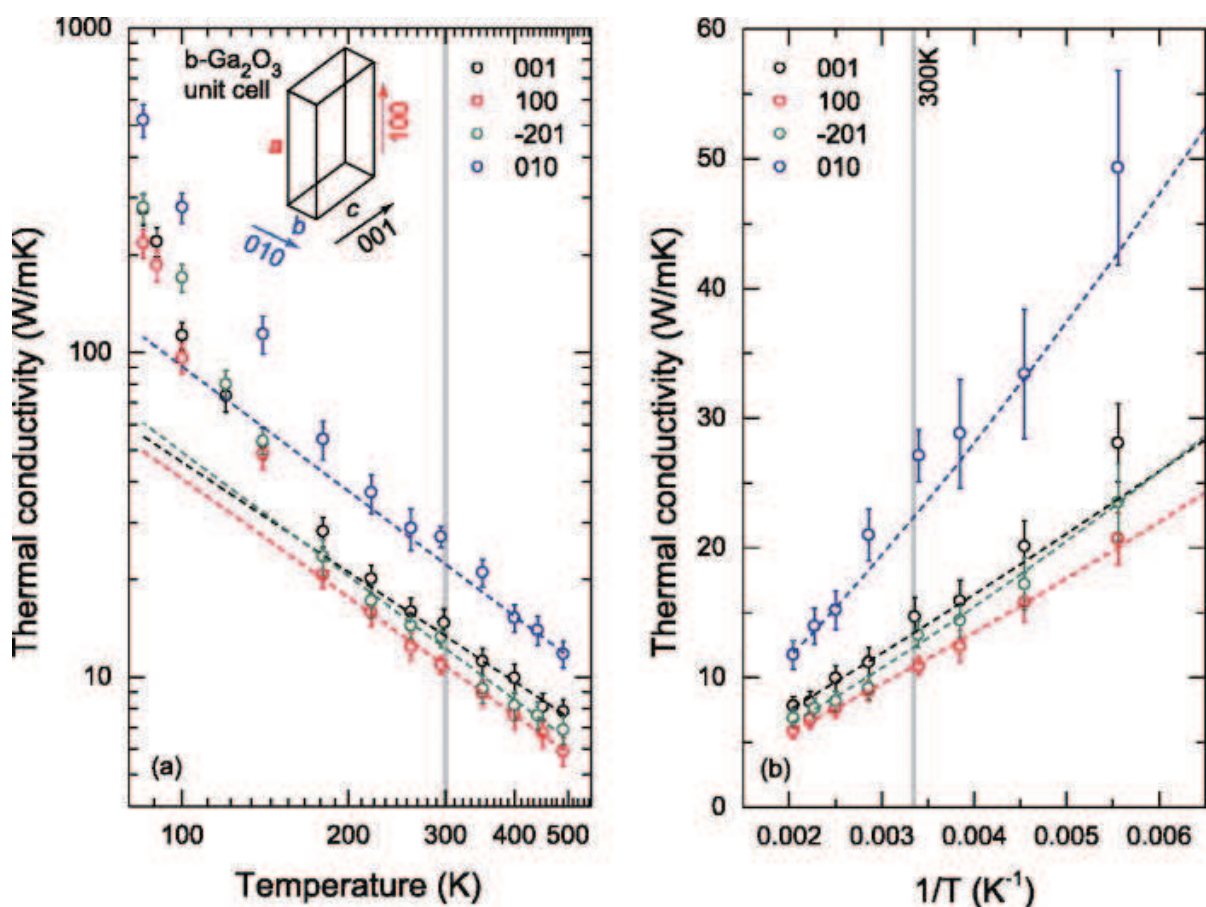

Figure 4. Thermal conductivity as a function of temperature for β-Ga_2O_3 along different crystal directions. (Reprinted with permission from Ref. [35]. Copyright 2015, American Institute of Physics.).

These studies showed that the spectra characteristic of undoped samples are independent of the excitation and emission wavelengths. However, the Si-doped sample produced a blue emission which was highly related to the excitation and emission wavelengths. Finally, it has been assumed that the red emission is caused by nitrogen impurities [32, 34].

2.3.3. Thermal properties

Ga$_2$O$_3$ is considered a weak thermal conductor compared to other semiconductors, with a thermal conductivity lower than that of other wide-bandgap materials such as SiC and GaN. Thermal conductivity in Ga$_2$O$_3$ varies depending on crystal direction due to its crystalline anisotropy. Directions with a smaller lattice constant have higher thermal conductivity., Ga$_2$O$_3$ has the highest thermal conductivity along the [010] direction and the lowest along the [100] direction. This has been measured at temperatures between 80 and 495 K (**Figure 4**). At high temperatures, thermal transport is primarily dominated by phonon scattering [35].

3. Ga$_2$O$_3$ nanowire growth mechanisms

A wide variety of methods have been used to grow Ga$_2$O$_3$ nanowires. These include thermal oxidation [36], vapor–liquid–solid mechanism [37], pulsed laser deposition [38], sputtering [39], thermal evaporation [40–42], molecular beam epitaxy [43], laser ablation [44], arc discharge [45], carbothermal reduction [46], microwave plasma [47], metalorganic chemical vapor deposition [48] and the hydrothermal method [49, 50]. **Table 3** summarizes the advantages and disadvantages of these methods. Research is ongoing to determine the best method for growing high-quality nanowires at low cost.

3.1. Thermal oxidation

Ga$_2$O$_3$ nanowires have been fabricated by oxidizing GaAs in a furnace [36]. At 1050°C and at atmospheric pressure, argon gas was used to grow Ga$_2$O$_3$ nanowires with a nanotextured surface. As the GaAs was heated, it dissociated and the arsenic evaporated, leaving behind a liquid Ga-rich surface which was then oxidized. At high temperatures, Ga$_2$O$_3$ nanowires began to grow. The roughness of the surface was believed to be caused by oxygen-deficiency defects and the difference in crystal structure between GaAs and Ga$_2$O$_3$.

When β-Ga$_2$O$_3$ nanowires are grown using this method, the material first begins as a thin film before nanowire formation if conditions are favorable. The steps in this process have been clearly described for GaAs oxidation in a furnace [51]. At high temperatures, phase separation of the GaAs occurs, and the constituents decompose. Arsenic diffuses through the substrate and evaporates from the surface, and gallium melts, forming clusters of liquid gallium on the surface. As the clusters form, the arsenic evaporates faster because it is easier for it to dissociate through the clusters than from the surface of the GaAs. Nanowire growth occurs from these clusters. Due to liquid Ga's ability to wet GaAs, the droplets are hemispherical. Oxygen in the chamber reacts with the Ga clusters to form a Ga$_2$O$_3$ thin film, with voids where the As evaporated. As the GaAs is converted into Ga$_2$O$_3$, Ga is no longer able to wet it, resulting in

Growth Mechanisms	Advantages	Disadvantages
Thermal oxidation	Simple and inexpensive	Low degree of control over growth
Vapor–liquid–solid	Good control of growth	Can interfere with doping levels
Pulsed laser deposition	High deposition rate	More defects and dislocations
RF magnetron sputtering	Non-stoichiometric deposition	• Incorporation of gas into material • It produces low quality NWs
Thermal evaporation	Inexpensive and compatible with many materials	Contamination of material
Molecular beam epitaxy	high deposition rate and low impurity levels	More surface roughness at higher temperatures
Laser ablation	High quality film	Expensive and require longer time
Arc-discharge	Faster growth	• Low quality NWs • Many defects
Carbothermal reduction	Simple process for growing a wide variety of structures	High levels of impurities
Microwave plasma	Can grow a wide variety of nanowires	Radial nonuniformity
Metalorganic chemical vapor deposition	High growth rate	Expensive and uses toxic gases
Hydrothermal method	Simple, cheap and efficient	Require precise temperature control
Sol-gel method	Simple and inexpensive	The thickness is nonuniform

Table 3. Advantages and disadvantages of β-Ga_2O_3 NWs growth techniques.

droplets with large contact angles. The droplets are unable to expand laterally and are thus forced to grow in one dimension, resulting in nanowire growth.

At oxidation temperatures above 750°C, nanowires begin to appear on the surface of Ga_2O_3 [51]. As the growth temperature is increased, the nanowires increase in length and density. The nanowires grown at 870°C (**Figure 5a**) were shorter and less dense than the ones grown at 900 and 942°C (**Figure 5b** and **c**). The samples were obtained by heating n-type (111) silicon-doped GaAs. **Figure 6** shows SEM images for nanowire growth at temperatures of 900, 1000 and
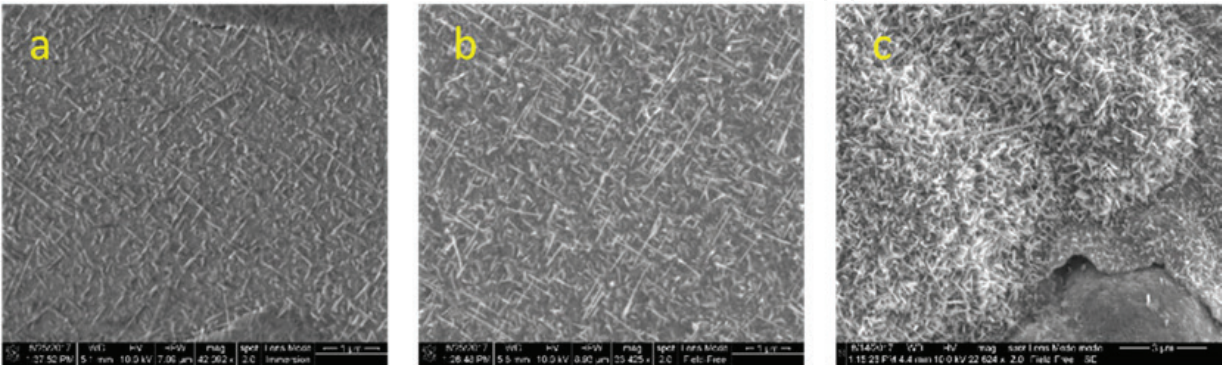

Figure 5. SEM images of n-type GaAs oxidized at (a) 870, (b) 900, (c) 942°C.
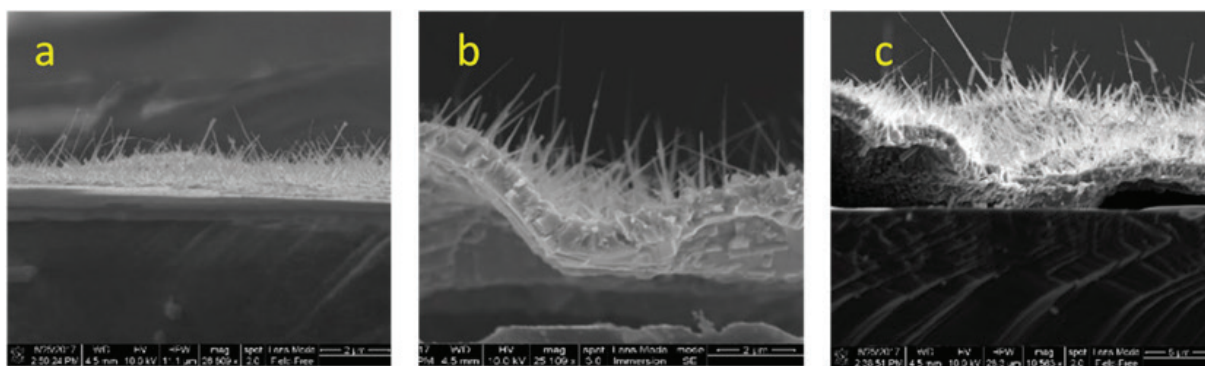
Figure 6. SEM image of cross-sections of GaAs oxidized at (a) 900, (b) 1000, (c) 1015°C.

1015°C. The average lengths of the nanowires were 1–2 μm for 900°C, 1–3 μm for 1000°C, and 2–4 μm for 1015°C. The differences in nanowire length caused by temperature are more apparent in these cross-sections. The nanowires are sharp and have apparently random orientations.

One problem seen with furnace oxidation is buckling and delamination of the Ga$_2$O$_3$ film on the surface, particularly at higher temperatures. This causes the orientation of the nanowires to be more random, as can be seen in **Figure 6**. Another problem with growing nanowires using thermal oxidation is that at some temperatures, the surface is not uniformly covered with nanowires but instead contains gallium clusters [51]. **Figure 7** shows focused ion beam (FIB) images of these bubbles on the surface that were formed at high temperatures due to the growth mechanism. If a nanowire device is used as a sensor, this means that the effective sensing surface area is reduced. The clusters could also negatively affect the performance of devices in other ways. This method is simple and inexpensive, but it does not allow precise control of nanowire growth, hence their lack of directionality.

3.2. Vapor–liquid–solid (VLS) approach

The VLS mechanism (**Figure 8**) is commonly used to grow nanowires. It requires the presence of impurities, which act as catalysts at the sites where nanowires will be grown [29]. The choice of impurity affects the diameter and growth direction of the nanowires and thus is an important growth parameter. Being impurities, the catalysts become part of the material and

Figure 7. (a) SEM image of a Ga cluster on the surface of n-type GaAs oxidized at 942°C, (b) Closeup of the same cluster after etching with a focused ion beam, showing nanowires surrounding the cluster but none on top of it.
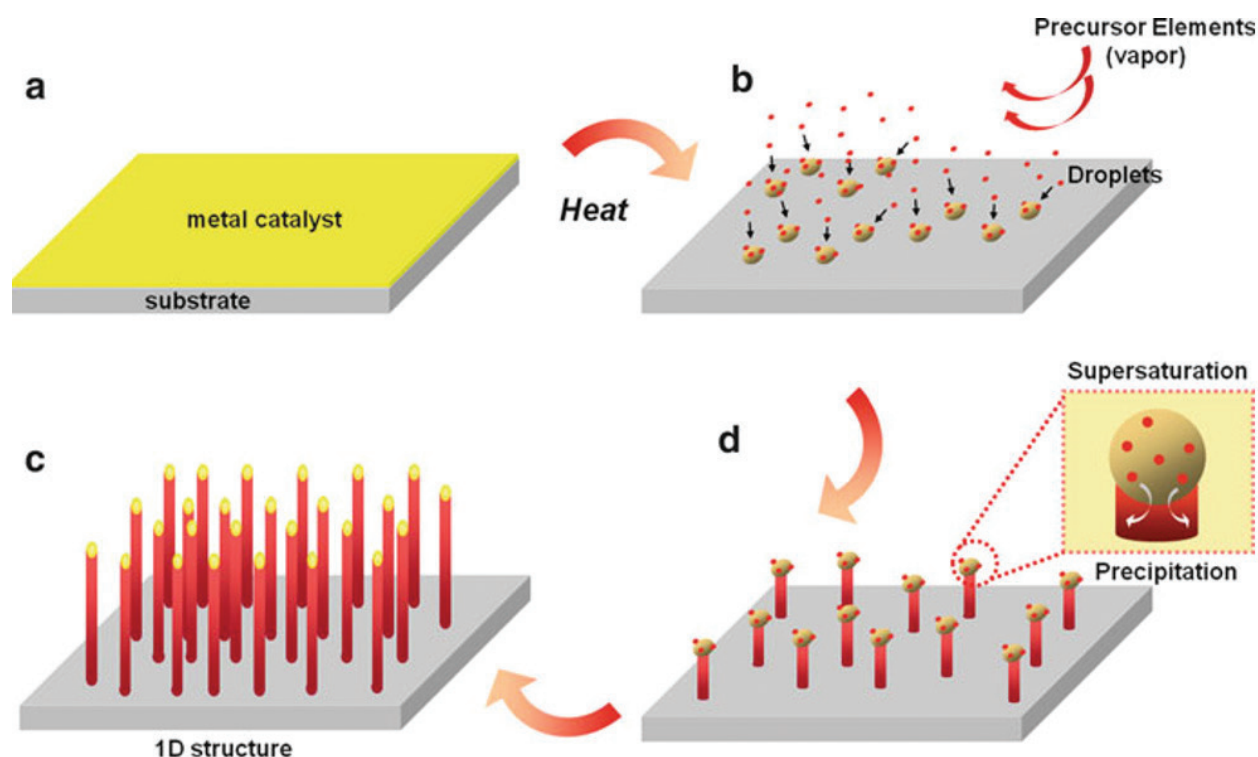
Figure 8. Vapor-liquid-solid growth of semiconductor nanowires.

can interfere with doping. Commonly used catalysts include Au, Ni, and Fe. These catalysts are commonly deposited on the substrate using the sol–gel method [37]. Nanowire growth occurs at the locations where the catalysts are deposited.

3.3. Pulsed laser deposition (PLD)

Pulsed laser deposition has been used to grow Ga_2O_3 nanostructures on α-Al_2O_3 at 900°C. The nanostructure was doped with Cr by alternating laser pulses to deposit both Ga_2O_3 and Cr [38]. This resulted in nanowires with a controlled length and diameter. The nanowires had tips larger than their bodies. PLD has a high deposition rate and is a low-cost growth method. There are many parameters involved in optimizing it for a specific process, such as the thickness of the catalyst, sample orientation, pulse intensity and number of pulses, and distance between laser and material, giving good control over the process. PLD produces more defects and dislocations due to the high energies used.

3.4. RF (radio frequency) magnetron sputtering

RF magnetron sputtering is another way of growing Ga_2O_3 nanowires [39]. If doping is needed, Ga_2O_3 powder can be mixed with the dopant (also in powder form) to form a sputter target. The fact that it produces non-stoichiometric films in an oxygen-deficient atmosphere is important in growing nanowires using Ga seeds. Growth time affects film thickness, which in turn affects the nanowires. The dopant only appears at the tip of the nanowires. Sputtering can be performed at room temperature, is low-cost, and provides good step coverage, but the films produced are not very high-quality because of damage caused during the process.

3.5. Thermal evaporation

Thermal evaporation has been used to grow Ga$_2$O$_3$ nanowires, mainly for gas-sensing applications [41, 42] at lower temperatures. In both cases, the nanowires were grown using a two-step process involving thermal evaporation and atomic layer deposition. This resulted in a Ga$_2$O$_3$ core and a different material (ZnO and SnO$_2$) as the shell on the outside, which acted as the sensor. The entire structure consisted of Ga$_2$O$_3$ nanowires that were coated with another material on the outside. The addition of the second material improves the performance of the gas sensors as compared to simply using Ga$_2$O$_3$ nanowires, mainly by lowering the temperature at which the sensor can operate. This method of growth is inexpensive and compatible with a wide variety of materials, but the evaporation process often leads to contamination by other substances present in the chamber.

3.6. Molecular beam epitaxy (MBE)

Molecular beam epitaxy is another option for growing Ga$_2$O$_3$. It has used to grow Ga$_2$O$_3$ on sapphire using both a Ga$_2$O$_3$ source and an elemental Ga source [43]. The pressure was less than 5×10^{-10} torr, and oxygen gas was used to protect the substrate from ions. For the Ga source, Ga was evaporated from an effusion cell through an oxygen plasma, while for the Ga$_2$O$_3$ source, Ga$_2$O$_3$ was evaporated from an iridium crucible with an oxygen plasma to decompose it into Ga$_2$O and O$_2$. Growth using elemental Ga required high temperatures to completely oxidize the Ga atoms, while with the Ga$_2$O$_3$ source, at lower temperatures, the oxide layer was thicker. Molecular beam epitaxy has also been used to grow Ga$_2$O$_3$ on β-Ga$_2$O$_3$ substrates [15]. The rate of growth was highly dependent on the substrate orientation, with the quickest growth occurring on the (010) and (310) planes and the growth on the (100) plane being very slow. At lower temperatures, surface roughness decreased. Molecular beam epitaxy has a high deposition rate and gives low impurity levels, but requires high temperatures and high vacuum conditions.

3.7. Laser ablation

Laser ablation involves the use of a laser on a Ga$_2$O$_3$ target to extract its contents and deposit them onto a substrate. Parameters such as pulse width, pulse power, distance between target and substrate, and the ablation target can all be controlled, giving this method high versatility and control over the material grown. The nanostructures it produces are high-quality but it takes a long time to grow them and it is expensive. For example, it took 5 hours to grow nanowires with diameters between 15 and 50 nm and lengths of several micrometers [52]. When a single nanowire was examined, it was found to be free of dislocations and stacking faults, attesting to the high quality of material that can be grown.

Laser ablation can also be used as part of a two-step process along with solution refluxing to grow Ga$_2$O$_3$ nanowires [53]. This approach allows nanowires to grow at the low temperature of 121°C. Rather than a Ga$_2$O$_3$ target, a high-purity Ga plate was used. While the time spent using the laser was only 20 minutes, the reflux process took a day, and calcination to convert the material grown into Ga$_2$O$_3$ took 18 hours, so this method requires more time to fabricate Ga$_2$O$_3$ nanowires.

3.8. Arc discharge

Arc discharge involves applying a direct-current arc voltage across an anode and cathode, both usually made of graphite, in an inert gas. The anode usually has a hole drilled into it to hold powders, which are used to grow the material desired, and the energy of the plasma generated is used to create nanostructures. In one study, the anode was a graphite electrode filled with GaN, graphite, and Ni powders while the cathode was a slightly larger graphite rod [45]. The growth took place in a helium environment. The Ni powder acted as a catalyst for the reaction. Nanostructures were deposited on the cathode, and most of them were nanorods. The nanorods were most commonly oriented in the [111] and [200] directions. Defects such as microtwins and stacking faults were found on some of the nanorods, suggesting that this method of growth does not produce very high-quality nanostructures.

A similar study has been carried out using a mix of Ni and Co powder as the catalyst inside the graphite anode and using a mixture of Ar and O_2 instead of He [54]. The pressure was varied, and it was found that no nanowires were present under 450 torr, suggesting that oxygen gas was necessary for their formation. Furthermore, without the Ni and Co powder there was no nanowire growth either. The nanowires obtained showed twin defects and rough step edges. The surfaces of the nanowires were covered with amorphous layers, and jog defects were also seen. Arc discharge can grow nanowires very quickly, but it produces nanowires that contain many defects.

3.9. Carbothermal reduction (CTR)

Carbothermal reduction is a simple method for growing Ga_2O_3 nanowires that involves mixing Ga_2O_3 and graphite powder and heating them in a furnace in the presence of a substrate [46]. This process can result in cactus-like nanostructures on the surface of the substrate. These nanostructures were very thin and had small spherical structures at their tips. Dense nanowire growth with a radial distribution was observed all over the surface of the samples. The cactus-like structures varied in diameter from a few micrometers to several tens of micrometers, which is much larger than conventional nanostructures. Nanowires with a vertical orientation were also seen, but their tips were often bent and a few had multiple nanorods with a random orientation at their tips. They were also tapered and had rough surfaces on closer examination. Growth time was correlated with nanowire density, and nanospheres were the first structures to grow on the surface, on top of which nanowires subsequently grew.

In another study, nanowires with lengths of tens of micrometers to hundreds of micrometers were grown using a similar process [29]. Different nanostructures were associated with different growth temperatures and substrates, with nanowires found at 900°C on Si substrates and nanosheets found at 800°C on quartz substrates. These nanosheets were large, with areas in the order of several tens of square micrometers. Their diffraction patterns were similar to that of thin films. When Si substrates were used at 800°C, Ga_2O_3 nanoribbons were observed. At high temperatures, the nanowires had sawtooth-like structures, which was believed to be due to oxygen deficiencies during growth. Although carbothermal reduction is a simple method

for growing Ga$_2$O$_3$ nanostructures and can be used to create a wide variety of structures, there are high levels of carbon impurities in the final material.

3.10. Microwave plasma

The microwave plasma method of growing nanowires involves using low-melting metals as a solvent medium for the growth of nanowires [47]. Droplets or thin films of gallium on the substrate cause nucleation of nanowires with high density (>10^{11} cm^{-2}). This technique was successfully used to grow unique "nanopaintbrushes." A variety of substrates were used with molten gallium and exposed to plasma in a microwave plasma reactor with H$_2$, CH$_4$, and O$_2$. After thin films developed, gallium droplets were added to grow nanowires. Stacking faults were not observed on the nanostructures. Four different nanostructures were seen on different parts of the substrate—nanowires, nanotubes, nanorods, and nanopaintbrushes—and it was suggested that the type of nanostructure formed depended on the initial state of the nuclei on the surface. Hydrogen appeared to etch the nuclei on the surface, preventing them from growing laterally and agglomerating with other nuclei, thus promoting vertical nanowire growth. This method of nanowire growth can produce a wide variety of nanostructures, but use of a plasma is associated with radial nonuniformity.

3.11. Metalorganic chemical vapor deposition (MOCVD)

Metalorganic chemical vapor deposition has been used to grow Ga$_2$O$_3$ nanostructures on Si/SiO$_2$ and Al$_2$O$_3$ [48]. As in furnace oxidation, nanostructures are only observed above a certain temperature (450°C in this case). The growth process consists of alternating pulses of a Ga precursor and H$_2$O and N$_2$ to purge the chamber. By changing the pulses of H$_2$O and using O$_2$, the morphology of the nanostructures can be controlled. With a longer pulse of H$_2$O, the nanowires were about a micron long and had large particles at their tips. If the water pulse was shortened, the wires would taper from the tip down, being widest at the tip and becoming thinner close to the substrate. At higher deposition temperatures, more nanostructures were observed on the surface. Metalorganic chemical vapor deposition provides relatively fast growth and high-quality films, but it is expensive and requires the use of highly toxic gases.

3.12. Hydrothermal Method

Ga$_2$O$_3$ nanowires can be obtained by calcination of gallium oxide hydroxide (GaOOH). This is considered the simplest method for growing β-Ga$_2$O$_3$ [49, 50]. The crystal of GaOOH is obtained when GaN reacts with different alkalis such as NaOH, NH$_4$OH, KOH, and Na$_2$CO$_3$ [49]. The GaOOH morphologies were changed into two different crystal structures: rhombohedral crystal (α-Ga$_2$O$_3$) and monoclinic crystal (β-Ga$_2$O$_3$). The morphologies of the gallium oxide were influenced by changing the temperatures [50]. **Figure 9** shows FE-SEM images of the GaOOH nanostructures grown by the hydrothermal method. Different growth temperatures were tried, such as room temperature, 50, 75, and 95°C. Temperature has a significant impact on the growth of gallium oxide. The number of shapes seen and the size of the nanowires increased as the temperature was increased. This growth method can be used at low temperatures.
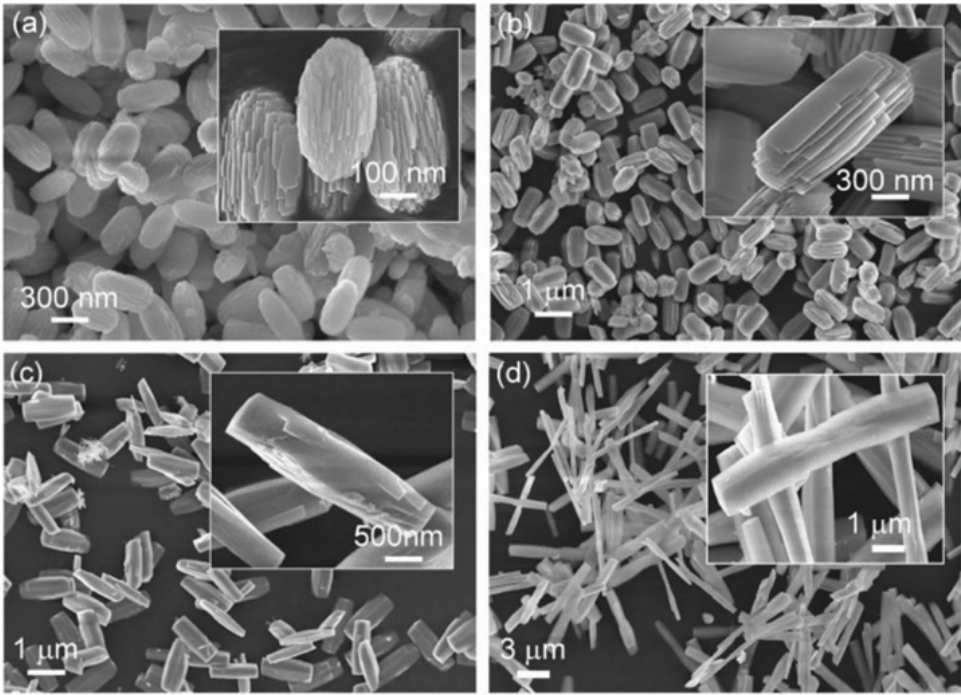
Figure 9. Effect of reaction temperature on the morphology of GaOOH nanostructures. Ref. [50] is licensed CC BY 4.0.

3.13. Ga2O3 growth substrates

Different substrates have been used to examine and produce low-cost and high-quality nanowires. The next sub-sections provide an overview of the substrates that have been utilized recently for the growth of gallium oxide nanowires. **Table 4** describes some advantages and disadvantages of different substrates on which β-Ga$_2$O$_3$ nanowires are grown.

Materials	Advantages	Disadvantages
Al$_2$O$_3$	Inexpensive and available	Lattice mismatch
GaN	Common and well-matched	Few defects observed
SiC	Large-scale fabrication processes	Lattice mismatch leads to high morphological and structural disorder
Ga$_2$O$_3$	Lack of lattice mismatch	Expensive and requires atmosphere with oxygen radicals to obtain a smooth surface.
MgAl$_6$O$_{10}$	Thermally stable Small lattice mismatch	Point defects: Oxygen vacancies, interstitial Ga, Ga vacancies and Ga-O vacancy pairs
MgO	It has wide bandgap and can shift the absorption edge to shorter wavelengths	Require annealing to improve crystallinity Oxygen vacancies
Si	Abundant & inexpensive	Lattice mismatch

Table 4. An overview of some substrates advantages and disadvantages were applied of β-Ga$_2$O$_3$ NWs growth techniques.

3.13.1. Aluminum oxide (Al$_2$O$_3$)

Al$_2$O$_3$ is one of the most commonly used materials for Ga$_2$O$_3$ growth. As sapphire is an insulator, this provides electrical isolation for Ga$_2$O$_3$. However, there is still lattice mismatch between the two materials. Lattice mismatches of 4.2% and 10.7% have been reported [44]. Sapphire is fairly inexpensive and available in different-sized wafers but there are always a few layers of α-Ga$_2$O$_3$ between a sapphire substrate and β-Ga$_2$O$_3$ [55]. It has also been reported that there is dissimilarity between the corundum crystal structure of sapphire and the monoclinic structure of β- Ga$_2$O$_3$ [56], but α-Ga$_2$O$_3$ has a corundum structure, so it is better-matched [57].

3.13.2. Gallium Nitride (GaN)

The lattices of GaN and Ga$_2$O$_3$ are well matched, and thus Ga$_2$O$_3$ is also commonly grown on GaN. ε-Ga$_2$O$_3$ keeps its morphology and has a low defect density when grown on GaN [55]. Furthermore, GaN has a wide bandgap, so using it as a substrate means that a photodetector will be less sensitive to longer wavelengths [58]. Both materials also have electron affinities of 4.0 eV, so there is almost no offset in the conduction band when Ga$_2$O$_3$ is grown on top of GaN.

3.13.3. Silicon carbide (SiC)

Depending on the orientation used, lattice mismatch between SiC and Ga$_2$O$_3$ can be fairly high [55]. When ε-Ga$_2$O$_3$ was grown on (001) SiC, morphological and structural disorder was very high, due to the difference between the crystal structures of the two materials, and the Ga$_2$O$_3$ was polycrystalline. Interestingly, in the [111] direction, high-quality Ga$_2$O$_3$ growth was observed. Because it is fairly easy to dope SiC, a p-n junction can be created using SiC as a substrate [59]. Using SiC as a substrate also enables fabrication of vertically structured devices because it is semiconducting.

3.13.4. Gallium oxide (Ga$_2$O$_3$)

Gallium oxide is also an occasionally used substrate for Ga$_2$O$_3$ growth. Due to the lack of lattice mismatch, high-quality crystal growth is possible [15]. To fully oxidize the gallium sub-oxides during pulsed laser deposition, an oxygen-radical-rich atmosphere is needed [60]. Without oxygen radicals, gallium tends to sublimate and its surfaces tend to be rough. Also, the high cost of Ga$_2$O$_3$ wafers makes them less attractive as a growth substrate.

3.13.5. Magnesium aluminum oxide (MgAl$_6$O$_{10}$)

As an alternative to using Al$_2$O$_3$, it is also possible to grow Ga$_2$O$_3$ on MgAl$_6$O$_{10}$. MgAl$_6$O$_{10}$ has high thermal stability and a lattice mismatch of only 2.9%, less than that of Al$_2$O$_3$ [44]. Chemically, the material is not very different from sapphire. When using MgAl$_6$O$_{10}$, several types of point defects in the Ga$_2$O$_3$ were observed, such as oxygen vacancies, interstitial Ga, Ga vacancies, and gallium-oxygen vacancy pairs. When MgAl$_6$O$_{10}$ is used, the donor band is formed by pairs of gallium vacancies and gallium-oxygen vacancies [61].

3.13.6. Magnesium oxide (MgO)

MgO has also been used as a substrate for growing Ga_2O_3. It tends to absorb water from the air, which affects the structural properties of the Ga_2O_3 on top [57]. When Ga_2O_3 is grown on MgO, it is initially amorphous and requires annealing to achieve good crystallinity [16]. However, this also decreases the bandgap, making the material less sensitive to UV light. The Ga_2O_3 film is also highly resistive, although it remains n-type due to oxygen vacancies.

3.13.7. Silicon (Si)

Ga_2O_3 can also be grown on silicon. It has been deposited on (100) Si [57]. A minimum temperature of 600°C was required for crystallization to occur. Because silicon, like silicon carbide, can be easily doped p-type, growing Ga_2O_3 on Si is an option to make a p-n junction. Ga_2O_3 grown on (100) Si using molecular beam epitaxy has good crystallinity and produces smooth surfaces [62].

4. Contacts for Ga_2O_3

Contacts to Ga_2O_3 can be either Schottky or ohmic. To make an ohmic contact, the barrier height of the metal should be low. Gold and titanium are the most commonly used metals for contacts. Metal contacts can be deposited using shadow masks, which involve depositing metal onto the substrate while it is covered by a thin plate with gaps in the desired shape.

4.1. Titanium/gold (Ti/Au)

Ti/Au interdigitated electrodes have been deposited on both β-Ga_2O_3 [63] and chromium-doped Ga_2O_3 nanowire thin films [38]. In both cases, a shadow mask was used and the contacts exhibited ohmic behavior. It was suggested that this was due to the abundance of surface states in Ga_2O_3, which makes it easy for carriers to tunnel.

4.2. Gold (Au)

A shadow mask has been used to deposit Au onto the back of a β-Ga_2O_3/Si heterojunction photodetector [62]. The deposition method was radio frequency magnetron sputtering. A Ti/Au contact was also sputtered on top of the β-Ga_2O_3. The contacts formed were ohmic. Standard photolithography techniques and liftoff have been used to deposit interdigitated Au electrodes on β-Ga_2O_3 [64]. Carrier multiplication that occurred in the area under the electrodes resulted in high responsivity and quantum efficiency.

4.3. Indium (In)

Thermal evaporation was used to deposit an In electrode on the SnO_2 part of a β-Ga_2O_3/SnO_2 heterojunction photodetector [65]. A bilayer of Ti and Au was also deposited on the β-Ga_2O_3 thin film using evaporation. The I-V curve of the device showed that the contacts were rectifying.

4.4. Titanium/aluminum (Ti/Al)

Electron beam evaporation was used to deposit Ti and Al onto the back side of a Ga$_2$O$_3$ photodiode [66]. On the other side of the diode, Schottky contacts of Au were also deposited. These contacts were rectifying. A contact consisting of alternating layers, Ti/Al/Ti/Al, was deposited through an interdigitated shadow mask onto a Ga$_2$O$_3$ photodetector [4]. The contacts were found to be non-ohmic, which was the goal.

4.5. Graphene

Graphene electrodes have also been deposited on a β-Ga$_2$O$_3$/SiC photodetector [67]. The graphene was grown by chemical vapor deposition on Cu and then transferred to the substrate. The graphene was transparent and thus allowed most incident light to reach the contact area. It also acted as a channel when the electrons and the holes were separated. On the back of the substrate, a Au/Ti electrode was deposited. A device with a gold electrode on top was also fabricated. The device with the graphene electrode showed a larger photoresponse, higher responsivity, larger I$_{light}$/I$_{dark}$ ratio, and a shorter rise time.

5. Ga$_2$O$_3$ nanowire applications

Ga$_2$O$_3$ nanowires, nanobelts and nanorods have been extensively studied in recent years. These Ga$_2$O$_3$ nanostructures provide a path to a new generation of devices, but most Ga$_2$O$_3$ nanostructure-based devices are limited to a single nanowire, and the integration of individual devices on a single chip is still a real challenge. Another crucial issue is controlled doping in nanostructures and the formation of high-quality ohmic contacts between nanostructures and electrodes. Therefore, the construction of a device via a simple and cost-effective method is still a great challenge. In spite of these difficulties, various Ga$_2$O$_3$ nanowire applications such as Ga$_2$O$_3$ nanowire-based FETs, gas sensors and UV photodetectors are reported.

5.1. UV photodetectors

The spectrum of radiation between 200 and 280 nm is called solar-blind due to the absorption of solar radiation in that spectrum by the ozone layer. Because of this lack of background noise, it is possible to detect very weak signals in this spectrum. In recent years, the need for solar-blind UV photodetectors has increased, due to their potential in several applications such as flame detection and missile warning [68]. When photons strike the surface of a UV photodetector, they generate electron–hole pairs. These electron–hole pairs change the conductivity of the material, which shows that light has been detected. For a device to detect signals in the UV spectrum, a material with a wide bandgap should be used. It is important that the material detect UV light but is not affected by light from other parts of the optical spectrum.

Photomultiplier tubes are used for UV detection in the solar-blind region, but they have several problems. They are bulky, require high bias voltages, and have high leakage current. Silicon-based photodiodes are also used, but due to their narrow bandgap, they require additional

filters to block light from unwanted parts of the optical spectrum. Wide-bandgap materials are preferred for use in solar-blind UV photodetectors because they are transparent to deep UV. Of the different materials available, Ga_2O_3 is particularly promising because of its wide bandgap of 4.9 eV, high melting point, and chemical stability.

5.2. Types of photodetector structures

Many different types of photodetectors can be made. Photoconductors, MSM photodiodes, Schottky diodes, p-n junctions, p-i-n junctions, and avalanche photodiodes have all been fabricated with Ga_2O_3.

5.3. Photoconductors

A photoconductor is basically a radiation-sensitive resistor. When a photon with more energy than the bandgap of the material is absorbed, an electron–hole pair is formed, which makes the material more conductive [69]. Photoconductors have a few key advantages, such as high internal gain at room temperature, large photoresponsivity, and lack of a need for amplifying equipment. They are also compatible with planar IC technologies [70], so it is not difficult to integrate them with other devices on a chip. However, a photoconductor has strong persistent photoconductivity, meaning that photocurrent persists even after removal of illumination [71]. In addition, the response speed is very slow, and the responsivity depends on the amount of time it is kept in the dark. It is not possible for a photoconductor to operate at zero bias, meaning that it consumes more power. Photoconductors also exhibit sublinear behavior for incident power [72] and poor contrast between UV and visible light.

5.4. MSM photodiode

MSM (metal–semiconductor–metal) photodiodes are a commonly used structure for Ga_2O_3 photodetectors. They consist of two back-to-back Schottky diodes with an interdigitated electrode on top of an active light-collecting region [69]. An MSM photodiode has fast operation due to a low capacitance per unit area. The speed of the device is limited by transit time rather than by RC time constant. Using electron beam lithography, electrode width and spacing can be made very small, improving the speed of the device. The device also has a simple structure that is easy to fabricate and integrate. However, there is intrinsic low responsivity due to the interdigitated electrodes covering the active region.

MSM photodiodes have high gain and are easy to integrate with read-out circuitry [73]. The interdigitated electrodes need to be close together to maintain device performance, but this lowers responsivity because it blocks part of the incoming light. It is also possible to illuminate the device from the back, but this makes fabrication much harder. Fabrication of an MSM photodiode requires only a single photolithography step [74] because it only needs a single active layer of dopants. The fabrication process is compatible with that of FETs, but fine feature sizes are required. It is difficult to reliably control the metal–semiconductor interface, and the reflection of light from surface metals is a problem. It is possible to make the dark current in an MSM photodiode very low [72]. The photoresponse is linear with optical power. There is good contrast between the visible and the UV spectrum, and the bandwidth is wide. However, noise is a significant problem [71] and the material has high resistivity [75].

5.5. Schottky photodiode

A Schottky diode consists of a metal layer in contact with a semiconductor layer that exhibits rectifying behavior due to the difference in the work function between the two layers [69]. It has high quantum efficiency, high response speed, and low dark current and exhibits good contrast between UV and visible light. A Schottky diode can operate at zero bias, and doping levels are important for controlling barrier height. Unlike photoconductors, Schottky diodes have a very low persistent photoconductivity [71]. However, a lack of uniformity in metal films leads to large leakage currents, and external quantum efficiency is reduced by transparent Schottky contacts. A back-illuminated Schottky contact does not have this problem, but those devices are more difficult to fabricate. Schottky diodes have a constant responsivity for excitations above the bandgap, independent of power and temperature [72], and the time response is limited by the RC time constant. They have some limitations. For example, the maximum responsivity is limited by reflection in the transparent top contact [75]. The leakage current of the contacts is strongly dependent on the Schottky barrier height, with a higher barrier corresponding to lower leakage current. Defects will also result in a large leakage current.

5.6. p-n photodiode

A p-n photodiode is a p-n diode made with materials that allow light to penetrate the p-n junction [69]. It has a fast response speed and low dark current, and can operate without an applied bias, so it consumes less power. The photoresponse is also linear with optical power [72]. For Ga$_2$O$_3$ devices, there is good rejection of light from the visible spectrum. The time response is limited by p-doping. A p-n photodiode can be either a homojunction, with both sides made of the same material, or a heterojunction, with different materials. Due to the difficulty of making p-type Ga$_2$O$_3$, only heterojunction photodiodes have been made, with materials such as Si [62] and SiC [59] used on the p side. With heterojunctions, it is possible to tune the bandgap of each material.

5.7. p-i-n photodiode

p-i-n photodiodes are similar to p-n photodiodes, except for the addition of an intrinsic layer between the p and n materials. In a p-i-n junction photodiode, absorbed photons generate electron–hole pairs, which are collected by the n and p layers due to the reverse bias. Carriers generated in the junction experience a high electric field and are separated rapidly, giving the detector a fast response [75]. The addition of an intrinsic layer improves absorption and increases the quantum efficiency. To reduce the capacitance, the thickness of the intrinsic layer can be increased. However, a thicker intrinsic layer increases the transit time [74]. The junctions are critical to device performance, because if recombination occurs in the junctions, device performance is degraded. There is a good UV-to-visible rejection ratio, sharp spectral responsivity cutoff, and fast response time.

5.8. Avalanche photodiode

An avalanche photodiode operates at high speeds and multiplies photocurrent internally, resulting in high sensitivity. Above the breakdown voltage, electron–hole pairs are accelerated by a

large applied field, causing impact ionization. The avalanche effect also amplifies noise. The gain changes with temperature as well as applied bias. Because large voltages are applied, the device consumes large amounts of power. There is no persistent photoconductivity [65] and the quantum efficiency is high. The detectivity and selectivity are also high, and the response and decay times are fast. An avalanche photodiode requires less chip area compared to other type of photodetectors [70], has high gain, and can operate with a high bandwidth. Its fabrication is also compatible with IC fabrication technology. There are uniform junction regions to handle high applied fields [75]. The thickness of the multiplication layer affects the electric field profile and spectral response.

5.9. Ga_2O_3 nanowire-based field ionization

The high aspect ratio of Ga_2O_3 nanowires gives them potential to be used as field emission devices [76, 77]. For this application, it is desirable for the material to exhibit emission at a low electric field and remain stable at high current densities [51]. The field enhancement factor is also an important figure of merit for determining whether a material is suitable for field emission. If a nanowire with a sharp tip and a high aspect ratio is used, there is a large electric field at the tip, which reduces the potential barrier for field emission and increases the field emission current. Ga_2O_3 nanowires with ultra-sharp tips 3.5 nm in radius (**Figure 10**) have been fabricated [51], demonstrating that Ga_2O_3 has potential in this area. In fact, the field emission characteristics of turn-on field, threshold electric field, and geometrical field enhancement factor of these nanowires were comparable to those of diamond nanostructures and single-wall carbon nanotubes.
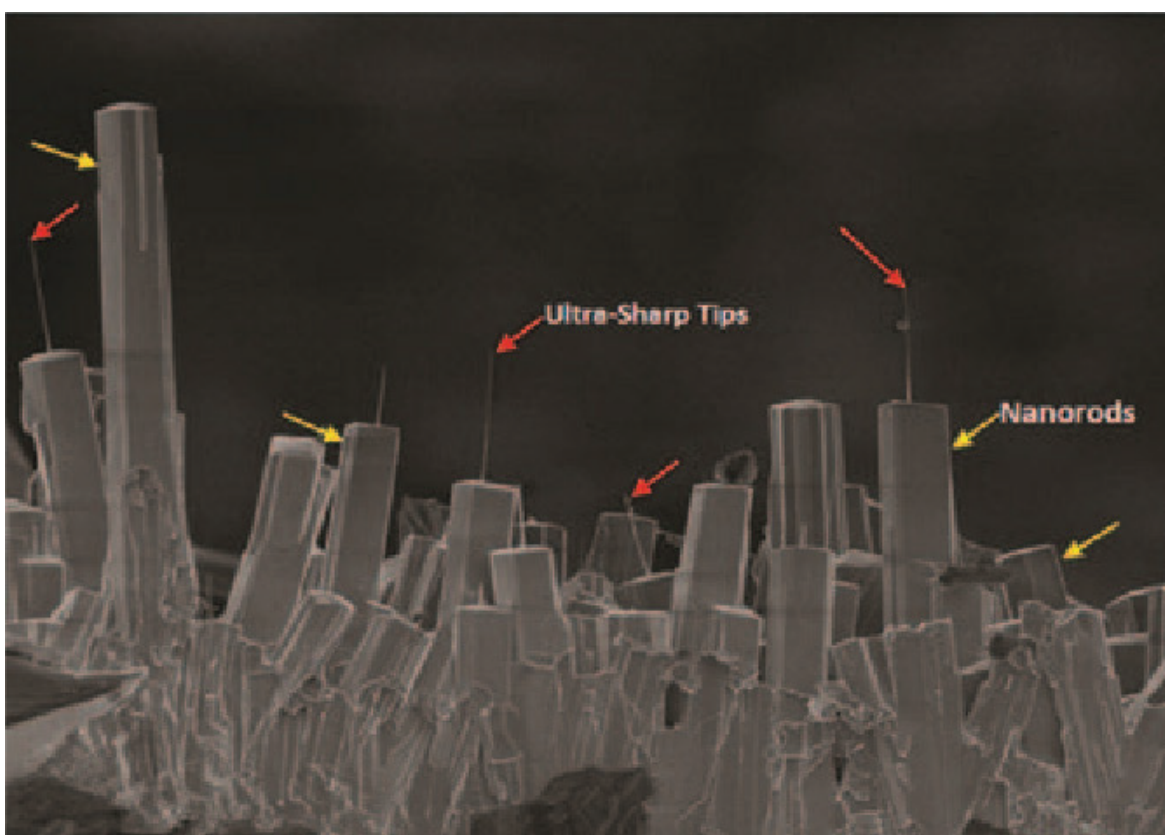

Figure 10. Transmission electron microscopy (TEM) image of the sharp tip. An ensemble of Ga or GaxO droplets is visible on the tip.

6. Ga$_2$O$_3$ FETs

A single Ga$_2$O$_3$ nanowire-based FET has been fabricated to measure the electrical properties of the as-grown nanowires [77, 78]. The device was fabricated on a silicon dioxide (SiO$_2$) film on top of an n-type silicon (Si) wafer with parallel pairs of Au contacts. These parallel Au electrodes acted as the source and drain, and an n-type Si layer served as the back gate. The Ga$_2$O$_3$ nanowires were first dispersed in ethanol, and then dried onto an n-type silicon chip. It was found that the conductance increased as the back-gate voltage increased. This suggests that the Ga$_2$O$_3$ nanowires had n-type characteristics, likely due to the presence of oxygen vacancies and extra gallium atoms in the lattice.

6.1. Ga$_2$O$_3$ nanowire-based temperature/gas sensor

β-Ga$_2$O$_3$ nanowire-based temperature sensors have unique conductivity behavior up to high temperatures. This property distinguishes this material from other semiconductors for nanodevice applications. Many studies have shown different methods for fabricating β-Ga$_2$O$_3$ nanowire-based gas sensors [5, 79, 80]. β-Ga$_2$O$_3$ appears to be an insulating material at room temperature; however, at high temperatures, it behaves as an n-type material and its conductance is greatly affected by its surroundings. To fabricate a gas sensor, Ga$_2$O$_3$ nanowires have been grown using the VLS method [80]. The developed sensor was cheap, easily fabricated and able to detect various chemical constituents at room temperature. As the target chemical substance approaches the nanowires, the gas may be physically adsorbed onto defects on the surface of the nanowire. This changes the dielectric constant of the nanowires, and the device detects the change in capacitance. As the concentration of the gas increases, the capacitance also increases. Because this sensor does not require an external heat source to recover quickly, it can operate at low power.

6.2. Photoelectrical generation of hydrogen

Ga$_2$O$_3$ nanowires show promise as a photocatalyst for splitting water into hydrogen and oxygen [81]. Efficiency was measured as 0.906%, much higher than the 0.581% efficiency of GaN thin films used for the same purpose. Ga$_2$O$_3$ is particularly attractive because of the tunability of its optoelectronic properties through doping and alloying, and enhancement of photoelectrochemical efficiency due to the presence of defect bands. However, when the nanowires were grown using a GaN substrate at high temperatures, an interfacial layer was observed between the nanowires and the GaN. This interfacial layer degraded the photoelectrochemical performance of the nanowires. Because the coverage of the substrate with nanowires is not complete, the substrate also contributes to the photoelectrochemical process.

7. Challenges & future perspectives

β-Ga$_2$O$_3$ nanowires have unique properties that distinguish them from other semiconductors. For instance, these nanowires have a wide bandgap and high chemical and thermal stability. Thus, Ga$_2$O$_3$ could be excellent for nanodevice applications in the future. However, a number of challenges associated with Ga$_2$O$_3$ still exist and need to be addressed.

7.1. Dopants

One issue is the introduction of specific dopants to enhance the electrical properties of nanowires. Specifically, a dopant that can reliably make Ga_2O_3 p-type needs to be found. More investigation is also required to evaluate the unintentional doping of Ga_2O_3 nanowires during their growth. The influence of these impurities on device performance also requires further study. Some procedural challenges for the growth of Ga_2O_3 nanowires also need to be solved. For instance, more directional Ga_2O_3 nanowire growth is highly desirable and the nanowires should also be more uniform in size and length. Finally, techniques to pattern and etch the Ga_2O_3 nanowires would be highly valuable.

7.2. Contacts

Different metals have been tested as contacts in Ga_2O_3 devices including titanium/gold, gold, indium, and graphene. These contacts are a key component in the performance of nanowire devices. Thus, more investigation into the ideal materials for ohmic and Schottky contacts in Ga_2O_3 nanowire devices is required. Integrating particular components of these nanowire devices to build a complete system at low cost is still a challenge. Research should also be performed on ways to improve carrier mobility and reduce contact resistance at the device level, and to lower costs to enable large-scale production.

7.3. Growth techniques

More research is required to identify the different factors that influence Ga_2O_3 nanowire growth and how these affect their optical, structural, thermal and electrical properties. Lattice mismatch needs to be taken into account when selecting a substrate for nanowire growth. High-quality fabrication at low cost for Ga_2O_3 nanowire growth is needed to make various nanowire devices such as FETs and UV photodetectors more attractive. The growth techniques for Ga_2O_3 nanowires should also be more closely examined to see if they can be improved on. Currently, different techniques such as molecular bean epitaxy (MBE), pulsed laser deposition (PLD), metal–organic chemical vapor deposition (MOCVD) and the hydrothermal method show promise in growing vertical Ga_2O_3 nanowires with high precision and control. Because Ga_2O_3 nanowires are a new material that has only recently been used in devices, integration of these devices with other devices on a chip is still necessary.

8. Conclusions

Ga_2O_3 nanowires exhibit unique electrical, thermal and optical properties that make them particularly attractive for use in future devices in sensing and optical applications. Using nanowires improves on the performance of thin films. These nanowires have a high surface-to-volume ratio, for high detection sensitivity. From a materials point of view, the wide bandgap of Ga_2O_3 also makes it less sensitive to visible light than other wide-bandgap materials such as GaN and SiC and allows it to handle higher power and temperatures. Thus, Ga_2O_3 nanowires are expected to play a key role in devices of the next generation.

Author details

Badriyah Alhalaili*, Howard Mao and Saif Islam

*Address all correspondence to: balhalaili@ucdavis.edu

Department of Electrical and Computer Engineering, University of California, Davis, USA

References

[1] Maier D, Alomari M, Grandjean N, Carlin JF, Diforte-Poisson MA, Dua C, et al. InAlN/GaN HEMTs for operation in the 1000 degrees C regime: A first experiment. IEEE Electron Device Letters. Jul 2012;**33**:985-987

[2] Tanaka A, Chen RJ, Jungjohann KL, Dayeh SA. Strong geometrical effects in submillimeter selective area growth and light extraction of GaN light emitting diodes on sapphire. Scientific Reports. Nov 27 2015;**5**:2

[3] Pearton SJ. GaN and Related Materials II. Australia: Gordon and Breach Science Publishers; 2000

[4] Weng WY, Hsueh TJ, Chang SJ, Huang GJ, Hsueh HT. A beta-Ga$_2$O$_3$ solar-blind photodetector prepared by furnace oxidization of GaN thin film. IEEE Sensors Journal. Apr 2011;**11**:999-1003

[5] Mazeina L, Perkins FK, Bermudez VM, Arnold SP, Prokes SM. Functionalized Ga$_2$O$_3$ nanowires as active material in room temperature capacitance-based gas sensors. Langmuir. Aug 17 2010;**26**:13722-13726

[6] Wang ZL. Nanowires and Nanobelts: Materials, Properties, and Devices. Boston: Kluwer Academic Publishers; 2003

[7] Geller S. Structure of beta-Ga$_2$O$_3$. Journal of Solid State Chemistry. 1977;**20**:209-210

[8] Ahman J, Svensson G, Albertsson J. A reinvestigation of beta-gallium oxide. Acta Crystallographica, Section C: Crystal Structure Communications. Jun 15 1996;**52**:1336-1338

[9] Lorenz MR, Woods JF, Gambino RJ. Some electrical properties of semiconductor beta-Ga$_2$O$_3$. Journal of Physics and Chemistry of Solids. 1967;**28**:403-&

[10] Villora EG, Shimamura K, Yoshikawa Y, Ujiie T, Aoki K. Electrical conductivity and carrier concentration control in beta-Ga(2)O(3) by Si doping. Applied Physics Letters. May 19 2008;**92**

[11] Varley JB, Weber JR, Janotti A, Van de Walle CG. Oxygen vacancies and donor impurities in beta-Ga$_2$O$_3$. Applied Physics Letters. Oct 4 2010;**97**(14):4-6

[12] Ahn S, Ren F, Oh S, Jung Y, Kim J, Mastro MA, et al. Elevated temperature performance of Si-implanted solar-blind beta-Ga$_2$O$_3$ photodetectors. Journal of Vacuum Science & Technology B. Jul 2016;**34**:4-7

[13] Tian W, Zhi CY, Zhai TY, Chen SM, Wang X, Liao MY, et al. In-doped Ga_2O_3 nanobelt based photodetector with high sensitivity and wide-range photoresponse. Journal of Materials Chemistry. 2012;**22**:17984-17991

[14] Matsuzaki K, Hiramatsu H, Nomura K, Yanagi H, Kamiya T, Hirano M, et al. Growth, structure and carrier transport properties of Ga_2O_3 epitaxial film examined for transparent field-effect transistor. Thin Solid Films. Feb 1 2006;**496**:37-41

[15] Higashiwaki M, Sasaki K, Kuramata A, Masui T, Yamakoshi S. Gallium oxide (Ga_2O_3) metal-semiconductor field-effect transistors on single-crystal beta-Ga_2O_3 (010) substrates. Applied Physics Letters. Jan 2012;**100**(1)

[16] Feng XJ, Li Z, Mi W, Luo Y, Ma J. Mg-doped beta-Ga_2O_3 films with tunable optical band gap prepared on MgO (110) substrates by metal-organic chemical vapor deposition. Materials Science in Semiconductor Processing. Jun 2015;**34**:52-57

[17] Cheng Y, Liang HW, Liu Y, Xia XC, Shen RS, Song SW, et al. Influence of N-2 and O-2 annealing treatment on the optical bandgap of polycrystalline Ga_2O_3:Cu films. Materials Science in Semiconductor Processing. Oct 2013;**16**:1303-1307

[18] Stepanov SI, Nikolaev VI, Bougrov VE, Romanov AE. Gallium oxide: Properties and applications – A review. Reviews on Advanced Materials Science. 2016;**44**:63-86

[19] Oshima T, Matsuyama K, Yoshimatsu K, Ohtomo A. Conducting Si-doped gamma-Ga_2O_3 epitaxial films grown by pulsed-laser deposition. Journal of Crystal Growth. Jul 1 2015;**421**:23-26

[20] Yan HY, Guo YR, Song QG, Chen YF. First-principles study on electronic structure and optical properties of Cu-doped beta-Ga_2O_3. Physica B: Condensed Matter. Feb 1 2014;**434**:181-184

[21] Wang XH, Zhang FB, Saito K, Tanaka T, Nishio M, Guo QX. Electrical properties and emission mechanisms of Zn-doped beta-Ga_2O_3 films. Journal of Physics and Chemistry of Solids. Nov 2014;**75**:1201-1204

[22] Dakhel AA, Alnaser WE. Experimental analysis of Ga_2O_3: Ti films grown on Si and glass substrates. Microelectronics Reliability. May 2013;**53**:676-680

[23] Zhang LY, Yan JL, Zhang YJ, Li T. Effects of N-doping concentration on the electronic structure and optical properties of N-doped beta-Ga_2O_3. Chinese Physics B. Jun 2012;**21**:8

[24] Liu LL, Li MK, Yu DQ, Zhang J, Zhang H, Qian C, et al. Fabrication and characteristics of N-doped beta-Ga_2O_3 nanowires. Applied Physics A: Materials Science and Processing. Mar 2010;**98**:831-835

[25] Zhang JG, Li B, Xia CT, Pei GQ, Deng Q, Yang ZH, et al. Growth and spectral characterization of beta-Ga_2O_3 single crystals. Journal of Physics and Chemistry of Solids. Dec 2006;**67**:2448-2451

[26] Villora EG, Yamaga M, Inoue T, Yabasi S, Masui Y, Sugawara T, et al. Optical spectroscopy study on beta-Ga_2O_3. Japanese Journal of Applied Physics Part 2-Letters. Jun 1 2002; **41**:L622-L625

[27] Harwig T, Kellendonk F, Slappendel S. Ultraviolet luminescence of beta-galliumsesqui-oxide. Journal of Physics and Chemistry of Solids. 1978;**39**:675-680

[28] Harwig T, Kellendonk F. Some observations on photo-luminescence of doped beta-gal-liumsesquioxide. Journal of Solid State Chemistry. 1978;**24**:255-263

[29] Kumar S, Singh R. Nanofunctional gallium oxide (Ga$_2$O$_3$) nanowires/nanostructures and their applications in nanodevices. Physica Status Solidi Rapid Research Letters. Oct 2013;**7**:781-792

[30] Geller S. Crystal structure of beta- Ga$_2$O$_3$. Journal of Chemical Physics. 1960;**33**:676-684

[31] Binet L, Gourier D. Origin of the blue luminescence of beta- Ga$_2$O$_3$. Journal of Physics and Chemistry of Solids. Aug 1998;**59**:1241-1249

[32] Song YP, Zhang HZ, Lin C, Zhu YW, Li GH, Yang FH, et al. Luminescence emission orig-inating from nitrogen doping of beta-Ga$_2$O$_3$ nanowires. Physical Review B. Feb 2004;**69**:9

[33] Shimamura K, Villora EG, Ujiie T, Aoki K. Excitation and photoluminescence of pure and Si-doped beta-Ga(2)O(3) single crystals. Applied Physics Letters. May 19 2008;**92**:9

[34] Chang LW, Lu TY, Chen YL, Yeh JW, Shih HC. Effect of the doped nitrogen on the optical properties of beta-Ga$_2$O$_3$ nanowires. Materials Letters. Jul 31 2011;**65**:2281-2283

[35] Guo Z, Verma A, Wu XF, Sun FY, Hickman A, Masui T, et al. Anisotropic thermal conduc-tivity in single crystal beta-gallium oxide. Applied Physics Letters. Mar 16 2015;**106**(11): 9-10

[36] Patil-Chaudhari D, Ombaba M, Oh JY, Mao H, Montgomery KH, Lange A, et al. Solar blind photodetectors enabled by nanotextured beta-Ga$_2$O$_3$ films grown via oxidation of GaAs substrates. IEEE Photonics Journal. Apr 2017;**9**:10-11

[37] Nguyen TD, Kim ET, Dao KA. Ag nanoparticle catalyst based on Ga$_2$O$_3$/GaAs semi-conductor nanowire growth by VLS method. Journal of Materials Science: Materials in Electronics. Nov 2015;**26**:8747-8752

[38] Guo DY, Wu ZP, Li PG, Wang QJ, Lei M, Li LH, et al. Magnetic anisotropy and deep ultraviolet photoresponse characteristics in Ga$_2$O$_3$: Cr vermicular nanowire thin film nanostructure. RSC Advances. 2015;**5**:12894-12898

[39] Lee SY, Choi KH, Kang HC. Growth mechanism of in-doped beta-Ga$_2$O$_3$ nanowires depos-ited by radio frequency powder sputtering. Materials Letters. Aug 1 2016;**176**:213-218

[40] Choi KH, Cho KK, Kim KW, Cho GB, Ahn HJ, Nam TH. Catalytic growth and structural characterization of semiconducting beta- Ga$_2$O$_3$ nanowires. Journal of Nanoscience and Nanotechnology. Jun 2009;**9**:3728-3733

[41] Park S, Sun GJ, Lee C. UV-assisted room temperature-gas sensing of Ga$_2$O$_3$-core/ZnO-shell nanowires. Journal of Ceramic Processing Research. Aug 2015;**16**:367-371

[42] Jang YG, Kim WS, Kim DH, Hong SH. Fabrication of Ga$_2$O$_3$/SnO$_2$ core-shell nanowires and their ethanol gas sensing properties. Journal of Materials Research. Sep 2011;**26**: 2322-2327

[43] Ghose S, Rahman MS, Rojas-Ramirez JS, Caro M, Droopad R, Arias A, et al. Structural and optical properties of beta- Ga_2O_3 thin films grown by plasma-assisted molecular beam epitaxy. Journal of Vacuum Science & Technology B. Mar 2016;**34**:10-14

[44] Feng Q, Li FG, Dai B, Jia ZT, Xie WL, Xu T, et al. The properties of gallium oxide thin film grown by pulsed laser deposition. Applied Surface Science. Dec 30 2015;**359**:847-852

[45] Han WQ, Kohler-Redlich P, Ernst F, Ruhle M. Growth and microstructure of Ga_2O_3 nanorods. Solid State Communications. 2000;**115**:527-529

[46] Cao CB, Chen Z, An XQ, Zhu HS. Growth and field emission properties of cactus-like gallium oxide nanostructures. Journal of Physical Chemistry C. Jan 10 2008;**112**:95-98

[47] Sharma S, Sunkara MK. Direct synthesis of gallium oxide tubes, nanowires, and nano-paintbrushes. Journal of the American Chemical Society. Oct 16 2002;**124**:12288-12293

[48] Pallister PJ, Buttera SC, Barry ST. Self-seeding gallium oxide nanowire growth by pulsed chemical vapor deposition. Physica Status Solidi A-Applications and Materials Science. Jul 2015;**212**:1514-1518

[49] Zhao YY, Frost RL, Yang J, Martens WN. Size and morphology control of gallium oxide hydroxide GaO(OH), nano- to micro-sized particles by soft-chemistry route without surfactant. Journal of Physical Chemistry C. Mar 13 2008;**112**:3568-3579

[50] Reddy LS, Ko YH, Yu JS. Hydrothermal synthesis and photocatalytic property of beta-Ga_2O_3 nanorods. Nanoscale Research Letters. Sep 16 2015;**10**:10-16

[51] Bayam Y, Logeeswaran VJ, Katzenmeyer AM, Sadeghian RB, Chacon RJ, Wong MC, et al. Synthesis of Ga_2O_3 nanorods with ultra-sharp tips for high-performance field emission devices. Science of Advanced Materials. Feb 2015;**7**(2):211-218

[52] Hu JQ, Li Q, Meng XM, Lee CS, Lee ST. Synthesis of beta-Ga_2O_3 nanowires by laser ablation. Journal of Physical Chemistry B. Sep 19 2002;**106**:9536-9539

[53] Huang CC, Yeh CS. GaOOH, and beta- and gamma-Ga_2O_3 nanowires: Preparation and photoluminescence. New Journal of Chemistry. 2010;**34**:103-107

[54] Park GS, Choi WB, Kim JM, Choi YC, Lee YH, Lim CB. Structural investigation of gallium oxide (beta- Ga_2O_3) nanowires grown by arc-discharge. Journal of Crystal Growth. Dec 2000;**220**:494-500

[55] Boschi F, Bosi M, Berzina T, Buffagni E, Ferrari C, Fornari R. Hetero-epitaxy of epsilon-Ga_2O_3 layers by MOCVD and ALD. Journal of Crystal Growth. Jun 1 2016;**443**:25-30

[56] Liu XZ, Guo P, Sheng T, Qian LX, Zhang WL, Li YR. Beta- Ga_2O_3 thin films on sapphire pre-seeded by homo-self-templated buffer layer for solar-blind UV photodetector. Optical Materials. Jan 2016;**51**:203-207

[57] Akazawa H. Formation of various phases of gallium oxide films depending on substrate planes and deposition gases. Vacuum. Jan 2016;**123**:8-16

[58] Nakagomi S, Sato T, Takahashi Y, Kokubun Y. Deep ultraviolet photodiodes based on the beta- Ga$_2$O$_3$/GaN heterojunction. Sensors and Actuators A-Physical. Aug 1 2015; **232**:208-213

[59] Nakagomi S, Momo T, Takahashi S, Kokubun Y. Deep ultraviolet photodiodes based on beta-Ga$_2$O$_3$/SiC heterojunction. Applied Physics Letters. Aug 12 2013;**103**:18-21

[60] Wakabayashi R, Oshima T, Hattori M, Sasaki K, Masui T, Kuramata A, et al. Oxygen-radical-assisted pulsed-laser deposition of beta-Ga$_2$O$_3$ and beta-(AlxGa1-x)(2)O-3 films. Journal of Crystal Growth. Aug 15 2015;**424**:77-79

[61] Mi W, Luan CN, Li Z, Zhao CS, Feng XJ, Ma J. Ultraviolet-green photoluminescence of beta- Ga$_2$O$_3$ films deposited on MgAl6O10 (100) substrate. Optical Materials. Oct 2013;**35**: 2624-2628

[62] Guo XC, Hao NH, Guo DY, Wu ZP, An YH, Chu XL, et al. Beta- Ga$_2$O$_3$/p-Si heterojunction solar-blind ultraviolet photodetector with enhanced photoelectric responsivity. Journal of Alloys and Compounds. Mar 5 2016;**660**:136-140

[63] Guo DY, Wu ZP, Li PG, An YH, Liu H, Guo XC, et al. Fabrication of beta-Ga$_2$O$_3$ thin films and solar-blind photodetectors by laser MBE technology. Optical Materials Express. May 1 2014;**4**:1067-1076

[64] Hu GC, Shan CX, Zhang N, Jiang MM, Wang SP, Shen DZ. High gain Ga$_2$O$_3$ solar-blind photodetectors realized via a carrier multiplication process. Optics Express. May 18 2015;**23**:13554-13561

[65] Mahmoud WE. Solar blind avalanche photodetector based on the cation exchange growth of beta-Ga$_2$O$_3$/SnO$_2$ bilayer heterostructure thin film. Solar Energy Materials and Solar Cells. Aug 2016;**152**:65-72

[66] Suzuki R, Nakagomi S, Kokubun Y, Arai N, Ohira S. Enhancement of responsivity in solar-blind beta- Ga$_2$O$_3$ photodiodes with a au Schottky contact fabricated on single crystal substrates by annealing. Applied Physics Letters. Jun 1 2009;**94**:19

[67] Qu YY, Wu ZP, Ai ML, Guo DY, An YH, Yang HJ, et al. Enhanced Ga$_2$O$_3$/SiC ultraviolet photodetector with graphene top electrodes. Journal of Alloys and Compounds. Sep 25 2016;**680**:247-251

[68] Zou RJ, Zhang ZY, Hu JQ, Sang LW, Koide Y, Liao MY. High-detectivity nanowire photodetectors governed by bulk photocurrent dynamics with thermally stable carbide contacts. Nanotechnology. Dec 13 2013;**24**:20

[69] Liu KW, Sakurai M, Aono M. ZnO-based ultraviolet Photodetectors. Sensors. Sep 2010;**10**:8604-8634

[70] Brennan KF, Haralson J, Parks JW, Salem A. Review of reliability issues of metal-semiconductor-metal and avalanche photodiode photonic detectors. Microelectronics Reliability. Dec 1999;**39**:1873-1883

[71] Sang LW, Liao MY, Sumiya M. A comprehensive review of semiconductor ultraviolet photodetectors: From thin film to one-dimensional nanostructures. Sensors. Aug 2013;**13**:10482-10518

[72] Monroy E, Calle F, Pau JL, Munoz E, Omnes F, Beaumont B, et al. AlGaN-based UV photodetectors. Journal of Crystal Growth. Sep 2001;**230**:537-543

[73] Qian LX, Liu XZ, Sheng T, Zhang WL, Li YR, Lai PT. Beta-Ga_2O_3 solar-blind deep-ultraviolet photodetector based on a four-terminal structure with or without zener diodes. AIP Advances. Apr 2016;**6**:21

[74] Berger PR. MSM photodiodes. IEEE Potentials. May 1996;**15**:25-29

[75] Alaie Z, Nejad SM, Yousefi MH. Recent advances in ultraviolet photodetectors. Materials Science in Semiconductor Processing. Jan 2015;**29**:16-55

[76] Huang Y, Wang ZL, Wang Q, Gu CZ, Tang CC, Bando Y, et al. Quasi-aligned Ga_2O_3 nanowires grown on brass wire meshes and their electrical and field-emission properties. Journal of Physical Chemistry C. Feb 5 2009;**113**:1980-1983

[77] Lin J, Huang Y, Bando Y, Tang CC, Li C, Golberg D. Synthesis of In_2O_3 nanowire-decorated Ga_2O_3 nanobelt heterostructures and their electrical and field-emission properties. ACS Nano. Apr 2010;**4**:2452-2458

[78] Li ZJ, Zhao B, Liu P, Zhang YF. Synthesis of gallium oxide nanowires and their electrical properties. Microelectronic Engineering. Jul 2008;**85**:1613-1615

[79] Jangir R, Porwal S, Tiwari P, Mondal P, Rai SK, Ganguli T, et al. Photoluminescence study of β- Ga_2O_3 nanostructures annealed in different environments. Journal of Applied Physics. 2012;**112**:034307

[80] Arnold SP, Prokes SM, Perkins FK, Zaghloul ME. Design and performance of a simple, room-temperature Ga_2O_3 nanowire gas sensor. Applied Physics Letters. Sep 7 2009;**95**:23

[81] Lam KT, Wu YL, Chang SJ. Photoelectrochemical hydrogen generation by Ga_2O_3 nanowires. Science of Advanced Materials. May 2017;**9**:810-814

[82] Higashiwaki M, Sasaki K, Kuramata A, Masui T, Yamakoshi S. Applied Physics Letters. 2012;**100**(1):3